Effect of Annealing on the Rheological and Thermal Properties of Aliphatic Hyperbranched Polyester Based on 2,2-Bis(methylol)propionic Acid

Ema Žagar,*,† Miroslav Huskić,† Jože Grdadolnik,† Majda Žigon,† and Andreja Zupančič-Valant‡

National Institute of Chemistry, Hajdrihova 19, SI-1000 Ljubljana, Slovenia, and Faculty of Chemistry and Chemical Technology, University of Ljubljana, Aškerčeva 5, SI-1000 Ljubljana, Slovenia

Received November 29, 2004; Revised Manuscript Received February 24, 2005

ABSTRACT: We investigated the effects of annealing on the rearrangement of H-bonding structure and its influence on the thermal and rheological properties of a fourth-generation hyperbranched polyester polyol based on 2,2-bis(methylol)propionic acid (Boltorn H40). With increasing annealing time and decreasing temperature, the enthalpy of the endothermic transition in the DSC thermograms of Boltorn H40 increases, whereas the viscoelastic response shows a considerable elastic contribution. During annealing of amorphous Boltorn H40, its structure becomes more ordered as a consequence of formation of multiple intermolecular H-bonds (−OH...O=C⟨ and/or −OH...−OH) between long linear sequences in the hyperbranched structure. DSC, FTIR, and XRD results of the individual fractions of Boltorn H40 and an ideally structured dendrimer analogue show that the ordering of the structure is highest in the case of low molar mass hyperbranched species with an open structure and low degree of branching. Such species have the longest average length of linear sequences between branch points and therefore the highest possibility for multiple H-bond interactions.

1. Introduction

Hyperbranched (HB) polymers are, like dendrimers, part of the family of multibranched or dendritic polymers. The building blocks of dendritic polymers are AB_x type monomers with one functional group A and x functional groups B reacting with each other. Dendritic polymers have a highly branched molecular architecture giving them macroscopic properties contrasting with those of their linear counterparts; differences in solubility, hydrodynamic volume, thermal, and rheological properties have been reported.[1−4] Therefore, dendritic polymers have attracted great scientific attention in recent years. The research so far has been focused mainly on the synthesis and characterization of various compositionally different families of dendritic polymers,[2,4−8] whereas a complete understanding of the interplay between their molecular architecture and macroscopic properties is still not unambiguous.

Dendrimers are well-defined, perfectly branched polymers and therefore monodisperse in molecular size and structure. Dendrimers in solutions of moderate and high concentrations, and in their melts, exhibit Newtonian behavior over a wide range of shear rates. The complex and steady shear viscosities are of equal values at the same deformation rate, frequency, or shear rate (the Cox−Merz rule). The zero-shear viscosity of dendrimer solution or bulk scaling with molar mass does not show the characteristic slope change, which is commonly associated with the critical chain length for entanglement formation.[2,5] These results support the suggestion that dendrimers do not engage in such physical interactions. The major disadvantage of dendrimers is their time-consuming stepwise synthetic route with low yields. This makes dendrimers rather costly to produce on a large scale.

From a large volume application standpoint HB polymers[9−11] are of greater interest since they can be produced on a large scale at a reasonable cost by one-pot or pseudo-one-pot reactions. However, such synthetic routes result in imperfect branching and a higher possibility of side reactions taking place. HB polymers also include partially reacted linear repeat units in their molecular structure, in addition to dendritic and terminal repeat ones, and are polydisperse with respect to molar mass and molecular structure. HB polymers have similar rheological and thermal behavior as dendrimers,[12,13] but the exact effect of their imperfectly branched structure and polydisperse character on their properties is not yet entirely clear.

One of the most widely investigated family of HB polymers are hydroxy-functional aliphatic hyperbranched polyesters, synthesized from 2,2-bis(methylol)propionic acid (bis-MPA) and various core molecules, either tris(methylol)propane or ethoxylated pentaerythritol[11,14−22] (commercially available Boltorn Hx polymers, where x denotes the pseudo-generation number, Perstorp Specialty Chemicals AB, Sweden). Studies on these compounds have included the kinetics of the poly(bis-MPA) formation,[14] the determination of structure (degree of branching, structures produced by side reactions: ether, cyclic),[15−18] molar mass averages, molar mass distribution, and investigation of poly(bis-MPA) dilute solutions[19−22] as well as their thermal,[11,13,19,23] rheological,[23−28] transport,[29] and dielectric relaxation properties.[30−32] The results of these studies show that poly(bis-MPA) HB polyesters are highly polydisperse in molar mass, composition (the content of dendritic, linear, terminal repeat units), and structure (with or without core molecule). The rheological behavior of thermally pre-

† National Institute of Chemistry.
‡ University of Ljubljana.
* Corresponding author: e-mail ema.zagar@ki.si, Fax +386 1 476 03 00.

10.1021/ma0475434 CCC: $30.25
Published on Web 03/31/2005

Scheme 1. Schematic Structure of H40 HB Polyester Based on Bis-MPA and a PP50 Core Molecule

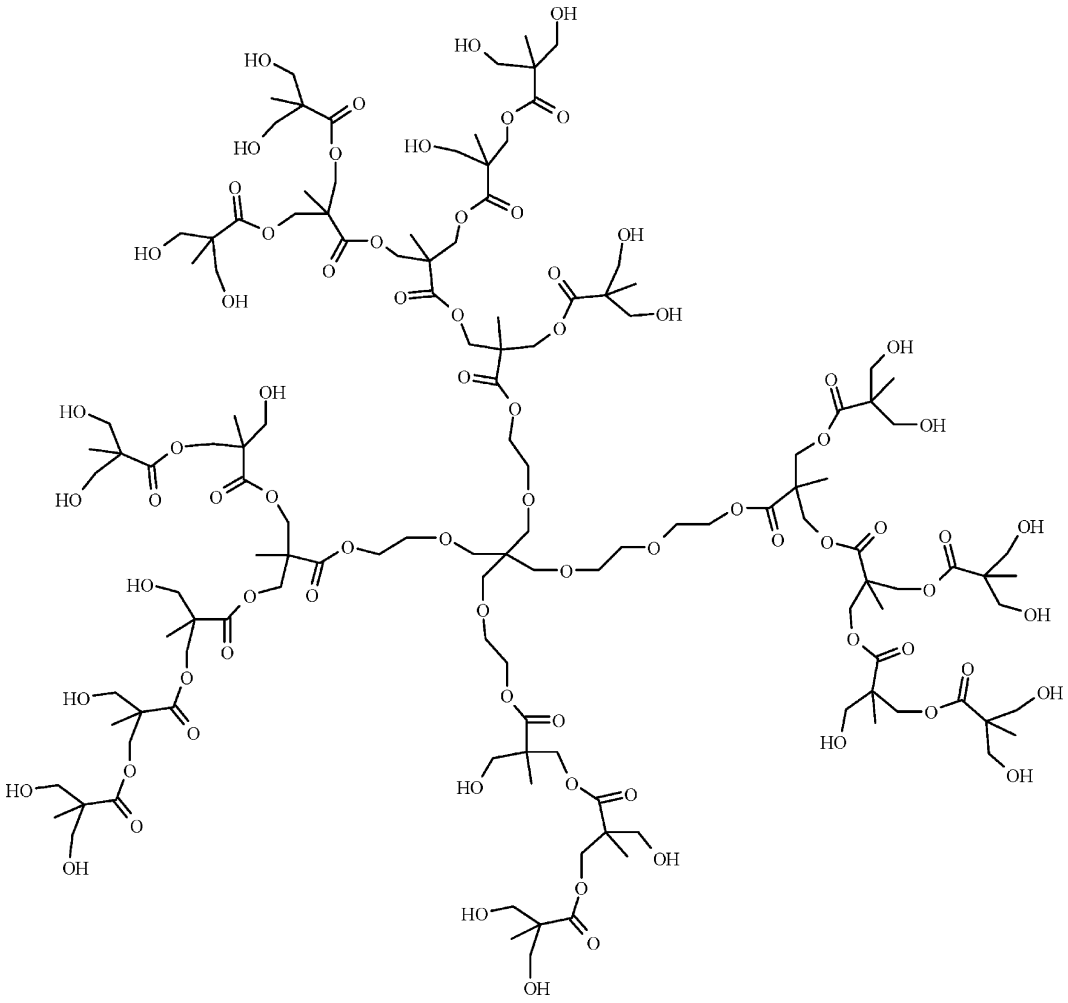

treated (20 MPa, 110 °C, 5 min, and then quenched samples) Boltorn H*x* HB polyesters in the molten state[1,2] depends on the generation number: the lower generation polyesters (second and third) demonstrate shear thinning behavior, whereas polyesters of fourth and fifth generation are Newtonian. Luciani et al.[13] reported that the rheological behavior of the fifth generation Boltorn polyester strongly depended on the thermal prehistory of the sample. The original sample stored at ambient temperature exhibited strong non-Newtonian behavior, which was ascribed to the microstructure that had developed as a consequence of physical aging involving hydrogen bonding of hydroxyl groups. After preheating the sample at 160 °C, the material showed Newtonian behavior. Shear thinning behavior of poly(bis-MPA) polyesters due to the aforementioned physical network structure has also been reported for the annealed samples at temperatures above their glass transition temperature (T_g).[28,33] A strong hydrogen-bonding network also results in an increase in the density of the solid by about 3%[13,28] and in a higher degree of structure ordering as revealed by a sharpening of the amorphous halo in the X-ray diffractometer scans of the annealed samples.[28] A very stable H-bond network at room temperature prevents poly(bis-MPA) HB polyesters from dissolving in various polar solvents on a molecular level unless the samples are thermally pretreated before the dissolution.[19] The cleavage of the secondary network of hydrogen bonding can be seen as an endotherm in DSC thermograms of poly(bis-MPA) HB polyesters.[13,19,28,33] The H-bond network in HB polyester Boltorn H40 was studied by infrared spectroscopy and by performing temperature measurements, hydration, and H/D exchange experiments.[34] It was found that the majority of hydroxyl groups are H-bonded, either to the carbonyl or hydroxyl groups, whereas other H-bond interactions are present, but to a minor extent.

The present work focuses on the effects of annealing a fourth-generation Boltorn H40 aliphatic HB polyester onto an H-bond network microstructure as studied by FT-IR spectroscopy and X-ray diffraction. The influence of H-bonding structure rearrangement on the thermal and rheological properties of Boltorn H40 was investigated by DSC and rheological measurements. The obtained results were further supported by thermal, spectroscopic, and XRD analysis of the dendrimer analogue and individual fractions of Boltorn H40.

2. Experimental Section

2.1. Materials. Boltorn H40 (Scheme 1) is a commercially available fourth-generation hydroxy-functional hyperbranched polyester synthesized from 2,2-bis(methylol)propionic acid (bis-MPA; AB_2) as the repeating unit and ethoxylated pentaerythritol (PP50; B_4) as the tetrafunctional core molecule (Perstorp Specialty Chemicals AB, Sweden). Our sample denotation is H40. H40 as an ideal dendrimer would theoretically have 64 primary end hydroxyl groups and a molar mass of 7316 g mol^{-1}. Because the growth of an HB polymer occurs randomly in a pseudo-one-step procedure, the structure of H40 includes fully reacted dendritic (D) and unreacted terminal repeat units (T) as well as partially reacted linear ones (L). The main side

Table 1. Content of Dendritic (D), Linear (L), and Terminal (T) Repeat Units, $\overline{DB}_{Frey}$, $\overline{DP}_n$, X, $\overline{M}_n$, x_{B_4}, x_{B_2}, the Average Number of OH Groups per Molecule, and the Fraction of Etherified Hydroxyl Groups for H40 and Its Fractions[a]

parameter	H40	F1	F3
D (%)	16.5	17.5	13.5
L (%)	57.0	59.0	58.0
T (%)	26.5	23.5	28.5
$\overline{DB}_{Frey}$	36.7	37.2	31.8
$\overline{DP}_n$	21.37	61.36	16.68
X	21.00	60.45	16.34
$\overline{M}_n$	2580	7340	2030
x_{B_4}	0.37	0.91	0.34
x_{B_2}	0.63	0.09	0.66
OH	22.97	62.82	18.36
OH_{ether} (%)	0.4	2.1	0.0

[a] The results are taken from ref 18.

reaction in the synthesis of H40 is the deactivation of bis-MPA carboxyl groups, leading to structures without a core molecule and with unreacted −COOH groups.[18] This side reaction lowers the number-average molar mass considerably ($\bar{M}_n$ = 2580 g mol^{-1}) compared to the theoretical molar mass, although the weight-average molar mass ($\bar{M}_w$ = 6640 g mol^{-1}) is only slightly influenced. Consequently, the molar mass distribution is broad (PDI = 2.6), and the sample contains high relative amounts of HB structures without a core molecule. Etherification and cyclization as side reactions are of minor importance.

The characteristics of H40 and its fractions obtained from ^{1}H and ^{13}C NMR spectra are given in Table 1. The fractions (F1, F3) of H40 were obtained by preparative SEC and show considerable differences in the composition, structure, $\overline{DB}$, and molar mass (Table 1).[18] $\overline{DB}_{Frey} = 2D/(2D + L)$[36] is the average degree of branching according to Frey, $\overline{DP}_n$ is the number-average degree of polymerization, X is the average number of bis-MPA molecules per one core molecule, M_n is a number-average molar mass, x_{B_4} and x_{B_2} are the fractions of structures with and without core molecule, OH is the average number of hydroxyl groups per one HB macromolecule, and OH_{ether} is the fraction of etherified −OH groups.

The dendrimer is a fourth-generation hydroxy-functional aliphatic polyester synthesized using 2,2-bis(methylol)propionic acid (bis-MPA; AB_2) as the repeating unit and 1,1,1-tris(hydroxyphenyl)ethane (B_3) as the trifunctional core molecule by a convergent growth approach. The theoretical molar mass of the dendrimer is 5526 g mol^{-1}, and it contains 48 end hydroxyl groups. It was kindly supplied by Prof. Dr. Andreas Hult, Royal Institute of Technology, Stockholm, Sweden.

2.2. Characterization. H40 and the dendrimer were dried in a vacuum oven at 50 °C for 24 h before measurements were taken. Fractions were collected by preparative SEC in *N*,*N*-dimethylacetamide (DMAc)[18] and were dried in a vacuum oven at 80 °C until the proton signals of *N*,*N*-dimethylacetamide (DMAc) in their ^{1}H NMR spectra disappeared.

2.2.1. Thermal characterization was carried out using a differential scanning calorimeter (DSC) Perkin-Elmer Pyris 1. The original sample was dried in a vacuum oven at ambient temperature for 3 days. In annealing experiments, the sample was heated to 150 °C (heating rate 10 °C min^{-1}) in order to remove the effect of sample thermal prehistory. It was then rapidly cooled (quenched: cooling rate 200 °C min^{-1}) to the predetermined temperature (50, 60, 70, 80, 90, and 100 °C). At each temperature the sample was annealed for different annealing times (from 0.5 h to 4 days). After annealing, the sample was quenched to −10 °C for 2 min to stabilize it and subsequently reheated to 160 °C at 10 °C min^{-1}. All analyses were performed under a nitrogen atmosphere.

2.2.2. Rheological Characterization. For rheological tests the sample was preheated for 15 min at 150 °C in order to break down the H-bond structure. After that the sample was cooled to the predetermined annealing temperature. This step was accomplished in 2 min. A controlled stress rheometer Haake RS150 equipped with a parallel plate sensor system 25 mm in diameter was used for all rheological measurements. Depending on the annealing temperature, the gap between the plates was set to either 1 or 1.25 mm. Time sweep tests under nondestructive conditions of oscillatory shear were performed at a constant frequency of 1 Hz. To perform the measurements under conditions of linear viscoelastic response (LVR) throughout the whole 3 h experimental time, tests were carried out at a constant strain amplitude of 3% from 90 to 70 °C and at 1% of strain amplitude at 60 °C.

2.2.3. FTIR Spectrometry. Infrared spectra were recorded on a Perkin-Elmer PE 2000 spectrometer equipped with a liquid nitrogen cooled MCT detector. On average 256 interferograms were collected and apodized using the Happ−Genzel function. The spectral resolution was 4 cm^{-1}. Thin layers of H40 were prepared from a methanol solution and were treated under dry nitrogen steam in order to remove all traces of methanol. The temperature measurements were performed using a diamond Golden Gate ATR cell (Specac). The temperature controller ensures the stabilization of the sample temperature to ±1 °C. Background spectra were collected for every recorded temperature to eliminate the effects of the intensity disparity of the diamond bands. The absorption spectra were calculated from optical constants. The optical constants, as well as related real and imaginary dielectric constants (ϵ' and ϵ'') were calculated using procedures proposed by Bertie and Eysel[37a] and Bertie and Lan.[37b] It should be noted that the number of reflections is not simply the actual number of reflections but also includes contributions from various type of approximations and neglected experimental factors such as beam convergence. The calculated number of reflections was 0.81. The spectra were recorded between 450 and 7000 cm^{-1}. The missing part of the spectrum between 0 and 450 cm^{-1} was replaced by the descending Gaussian function. The films were heated to 150 °C, subsequently cooled to either 50 or 90 °C, and tempered for 24 h. The variations in spectra were monitored by difference spectroscopy. The vibrations of CH_3 and CH_2 groups were used as indicators for proper subtraction. Because these groups are unaffected by the reappearance of the H-bond structure, the bands of these vibrations should be absent in the difference spectrum.

2.2.4. X-ray Diffraction (XRD). XRD experiments were performed using a Philips 17-10 diffractometer with Cu Kα radiation (λ = 1.54 Å). The scattering intensities were detected using a scintillation counter with an angular range of 2°−35° (in 2θ), an angular step of 0.04°, and a measurement time of 1 s per step.

3. Results

3.1. Characterization of Boltorn H40 HB Polyester. 3.1.1. Thermal Characterization. Boltorn H40 is an amorphous polymer with a glass transition temperature (T_g) at around 31 °C (Figure 1). The shape of its DSC trace strongly depends on the sample thermal history, i.e., cooling rate, annealing temperature, and annealing time.

The effect of cooling rate ($0.5 \le q_c \le 200$ °C min^{-1}) on the sample second heating DSC thermogram is shown in Figure 1.

Similarly to amorphous polymers, an endothermic peak is superimposed on the classical C_p step inherent to the glass transition.[38,39] The magnitude of this peak increases with decreasing cooling rate. This peak represents an indirect measure of the relaxation of enthalpy during the physical aging process that ensures the cohesion of the glassy state. Above T_g, the DSC curve of the quenched sample (cooling rate 200 °C min^{-1}) shows a broad exothermic peak centered at around 72 °C followed by a small broad endothermic peak, which extends up to a temperature of 140 °C. The enthalpy (ΔH) of these transitions could not be accurately deter-

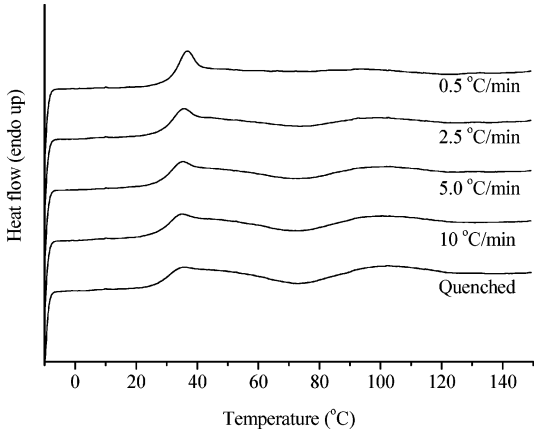

Figure 1. DSC curves of H40 (heating rate 10 °C min^{-1}) after various cooling rates ($0.5 \leq q_c \leq 200$ °C min^{-1}).

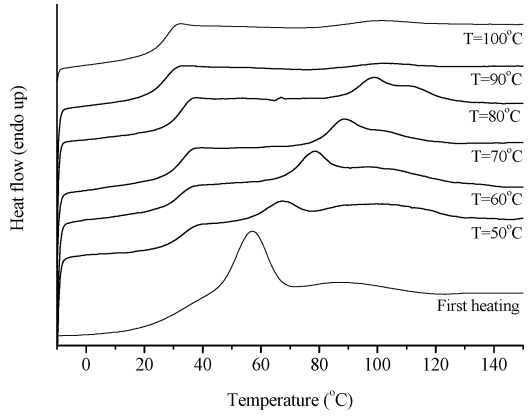

Figure 2. DSC curves of original H40 (first heating) and H40 annealed for 1 h at the indicated temperatures.

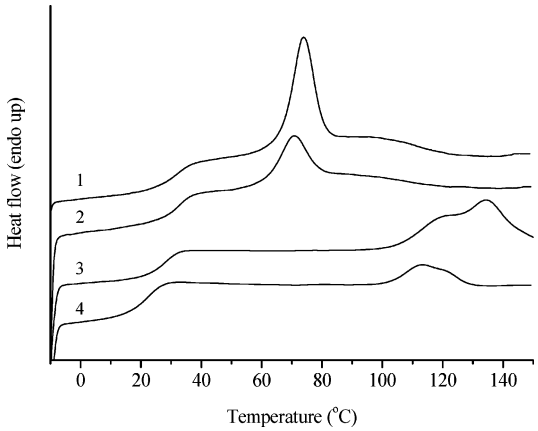

Figure 3. Influence of the annealing time and annealing temperature on the DSC curves of H40. 1: 50 °C, 48 h; 2: 50 °C, 4 h; 3: 90 °C, 48 h; 4: 90 °C, 4 h.

mined since the two peaks are not well resolved. The intensity of both peaks decreases as the cooling rate is lowered. Since the end-capped HB polymer does not show either physical aging effects or exo- and endothermic transitions, it has been suggested that hydrogen bonding associated with the large number of hydroxyl groups in H40 is responsible for the observed thermal behavior of the sample.[13,19,28,33] The FTIR thermal analysis of annealed H40 shows that the endothermic peak is accompanied by a pronounced frequency change in the OH stretching band.[34] A detailed analysis of FT-IR spectral parameters (frequency, bandwidth, band area, and band shape) of all possible proton acceptor groups indicates that this frequency jump is mainly a consequence of the weakening of H-bonds between hydroxyl groups.[34] The H-bonds between hydroxyl and carbonyl groups appear to be too weak to be detected by DSC. In addition, −OH...O=C⟨ H-bonds weaken continuously with rising temperature. Therefore, the exothermic peaks in thermograms of H40 are ascribed to the formation of H-bonds between hydroxyl groups, whereas the endothermic peaks above 70 °C are ascribed to their cleavage. In all corresponding cooling scans, no peaks were visible and no clear T_g could be detected.

In annealing experiments, the formation of H-bonds depends on annealing temperature and annealing time. The enthalpy change in isothermal H-bond formation is relatively small and cannot be directly monitored by isothermal DSC measurements. Better results were obtained by determination of H-bond cleavage enthalpy from the heating scans of the annealed H40. Figure 2 represents the DSC curves of the original H40 and of H40 annealed for 1 h at different temperatures. The original sample shows strong endothermic relaxation, which is superimposed on its glass transition and extends up to about 120 °C. In the DSC thermograms of the annealed H40 (50−80 °C) the endothermic peak shifts toward higher temperatures with increasing annealing temperature, whereas the enthalpy at this transition decreases. The DSC curves of the sample annealed at 90 and 100 °C exhibit a small exothermic peak above T_g.

The whole peak also shifts toward higher temperatures with increasing annealing time, but in this case the enthalpy of the transition increases (Figure 3). Therefore, the formation of H-bonds at a given temperature is more extensive at longer annealing times. Such behavior is similar to the isothermal crystallization of semicrystalline polymers.[40,41] The endothermic transition seems to be composed of two poorly resolved peaks. When H40 was annealed at lower temperatures (50−80 °C), the intensity of the low-temperature peak prevails at the end of the annealing process, whereas at higher temperatures (90−100 °C) the high-temperature peak is dominant.

The enthalpy (ΔH) associated with this transition increases with increasing annealing time and decreasing annealing temperature (Figure 4). An exception is the ΔH determined at 90 °C for long annealing times (above 24 h) since the values are larger than those determined at 80 °C.

The kinetics of H-bond formation in H40 can be adequately described by crystallization kinetics, i.e., by a nucleation and growth ordering mechanism. This mechanism has also been used to describe the ordering process in amorphous block copolymers.[42] The first step in H-bond formation seems to be a homogeneous nucleation; the rate (N) per unit volume and time can be described by eq 1.[43]

$$N = N_0 e^{-(E_D/RT)} e^{-(\Delta G^*/RT)} \quad (1)$$

where N_0 is a constant, ΔG^* is the free energy of formation of stable nucleus, and E_D is the transport energy. The first exponent of the equation expresses a retardation of nucleation due to the viscosity effect. Because ΔG^* is a function of temperature, the nucleation rate is also a function of temperature. The

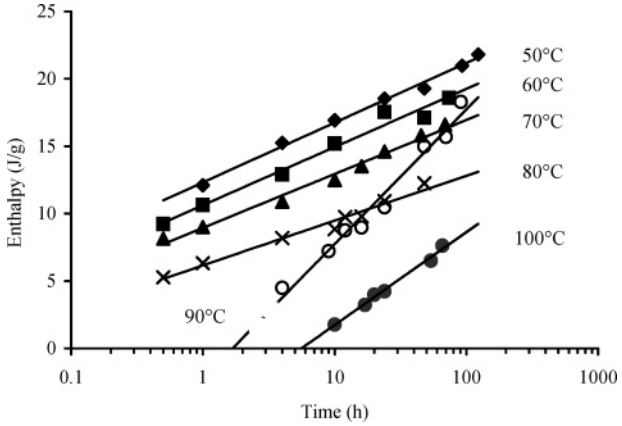

Figure 4. H-bond cleavage enthalpy, ΔH, of H40 as a function of annealing time for different annealing temperatures. ΔH for 0.5 h at 50 °C and for 1 h at 90 °C are missing since the presence of the small exotermic transition in DSC thermograms of such annealed H40 does not allow a reliable ΔH determination.

Table 2. Kinetic Data (ΔH_0, K, Eq 2) for the H-Bond Formation Process in H40

temp, °C	ΔH_0, J g^{-1}	k	temp, °C	ΔH_0, J g^{-1}	k
50	12.3	1.92	80	6.2	1.44
60	10.6	1.87	90	−1.6	4.10
70	8.9	1.74	100	−5.2	3.00

nucleation rate of H40 is zero at temperatures above about 140 °C and at absolute zero, while a maximum value is reached at an intermediate temperature. At 50 °C, which is only 20 °C above T_g, the viscosity of the melt is high, and therefore the first part of eq 1 is dominant. As a consequence, the induction time is long, and thus the ΔH at the annealing time of 0.5 h cannot be reliably determined. On the other hand, the number of created nuclei was the highest at 50 °C, and consequently, at annealing times above 1 h, the determined ΔH values are largest. At higher temperatures (90, 100 °C), the melt viscosity and nucleation rate are low. For that reason, ΔH can be reliably determined only at annealing times longer than either 4 or 10 h. On the other hand, the rate of H-bond formation is faster at higher temperatures, which is evident from the steeper slopes of the straight lines at 90 and 100 °C shown in Figure 4.

The ΔH of H-bonds cleavage increases linearly with the logarithm of annealing time according to eq 2 (Figure 4, Table 2).

$$\Delta H = \Delta H_0 + k \ln(t) \qquad (2)$$

where ΔH is the enthalpy of the H-bond cleavage, ΔH_0 is the enthalpy of H-bond cleavage at $t = 1$ h, k is the slope of the straight line representing the rate of H-bond cleavage, and t is the annealing time (h). The same dependence of ΔH on annealing time was also observed in secondary crystallization or annealing of semicrystalline polymers at high or ambient and subambient temperatures.[44−46] At temperatures from 50 to 80 °C, ΔH_0 and the constant k decrease with increasing annealing temperature. These results are in agreement with the results for secondary crystallization at high temperatures.[44,45] At 90 and 100 °C, a sudden increase in constant k was observed, whereas ΔH_0 had a negative value.

The annealing of H40 at temperatures between 50 and 100 °C has a small effect on sample T_g, but a much larger one on the heat capacity (ΔC_p) at the glass transition. ΔC_p decreases with increasing ΔH (Figure 5), indicating a restricted molecular mobility due to extensive H-bond structure formation. The decrease in ΔC_p at the glass transition at a higher degree of crystallization (ΔH) has also been observed for semicrystalline polymers.[47]

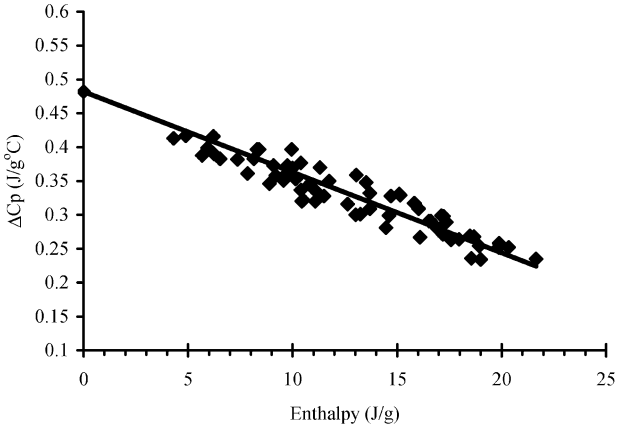

Figure 5. Dependence of heat capacity, ΔC_p, at glass transition on ΔH for H40.

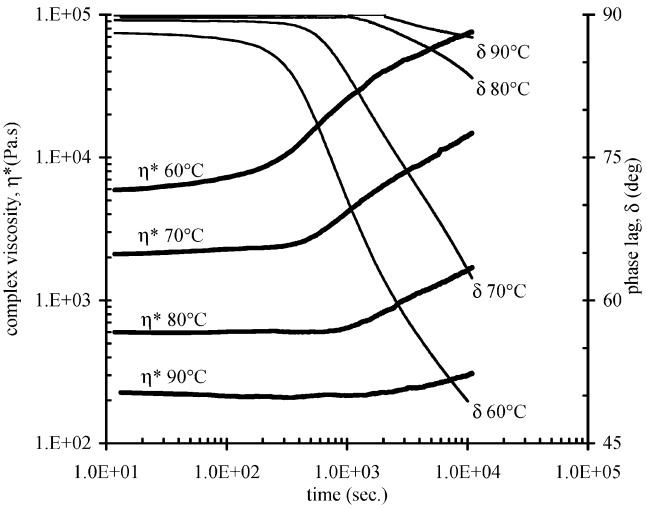

Figure 6. Influence of annealing time on complex viscosity and phase lag under nondestructive conditions of oscillatory tests at a frequency of 6.28 rad/s under the conditions of LVR for the investigated H40 at 60, 70, 80, and 90 °C.

3.1.2. Rheological Characterization. The changes in macroscopic properties due to structural buildup through the formation of H-bonds in H40 during annealing were followed by measuring the complex viscosity (η^*) and the phase lag (δ) at different annealing temperatures (60, 70, 80, and 90 °C; Figure 6). At 60 °C, a slight increase in η^* was already noticed at the beginning of the annealing. A pronounced increase in η^* starts after about 200 s, indicating that the process of extensive H-bond formation has begun to take place. The same behavior of η^* was also observed at 70 °C; only that the induction time for extensive H-bond formation process is longer, 500 s. At 80 and 90 °C, η^* remains constant for 1000 and 2000 s, respectively, and after that structure formation begins (Figure 6).

At lower temperatures (60, 70 °C), the phase lag was already slightly lower than 90° at the beginning of the annealing process, meaning that H40 exhibits viscoelastic behavior with a predominant viscous contribution

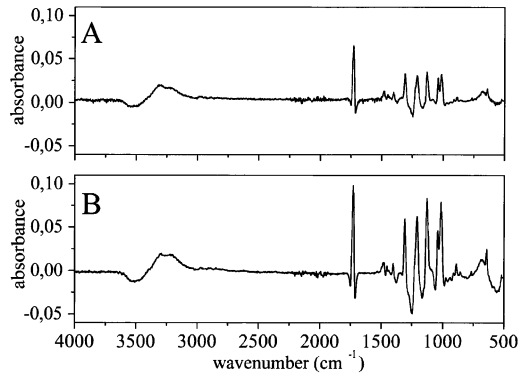

Figure 7. Difference FT-IR spectra of H40 obtained by subtraction of FT-IR spectra recorded at the end and at the beginning of the annealing process at temperatures of 90 °C, 24 h (A) and 50 °C, 24 h (B).

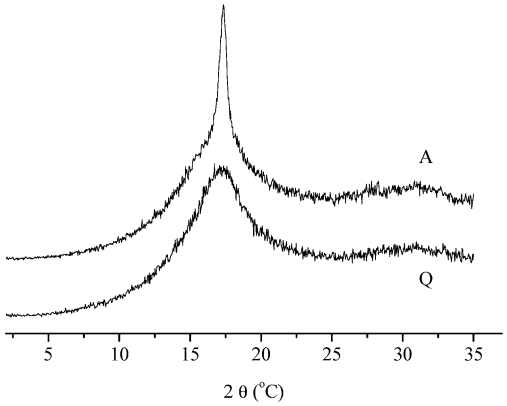

Figure 8. X-ray diffractograms of quenched and annealed H40 HB polyester: Q = quenched H40; A = annealed H40 at 50 °C for 14 days.

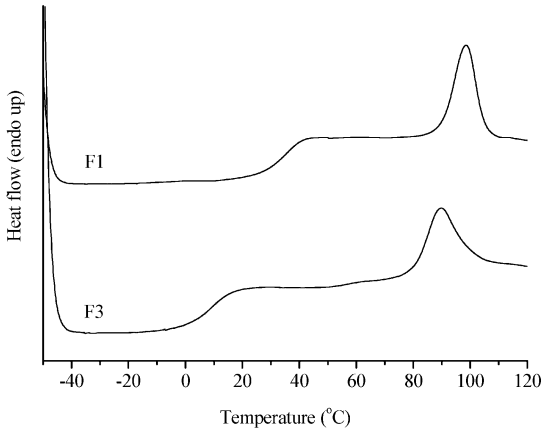

Figure 9. DSC curves of fractions F1 and F3 annealed at 80 °C for several days.

(Figure 6). At these temperatures some of the H-bonds must have already been formed while cooling the sample down from 150 °C to the annealing temperature, i.e., before the rheological tests were performed. During annealing a pronounced decrease in the phase lag was observed as a consequence of extensive H-bond formation. At higher annealing temperatures (80, 90 °C) the phase lag before the onset of structure formation was 90°, indicating that H40 exhibits only viscous behavior. When the H-bond formation process starts (above 1000 s at 80 °C and 2000 s at 90 °C), the phase lag starts to decrease. The deflection of phase lag accounts for increasing elastic contribution to the viscoelastic response of the sample as a consequence of an increasing number of formed H-bonds. The deflection of phase lag is more pronounced at lower annealing temperatures (60, 70 °C), which is in agreement with the obtained DSC results.

3.1.3. FTIR Spectrometry. The complete assignment of the bands in the infrared spectrum of H40 is given in our previous paper.[34] At this time, changes in the difference spectra recorded at the end and at the beginning of the annealing process at temperatures of 50 and 90 °C are shown (Figure 7).

The difference spectra show only the groups that are a donor or acceptor of hydrogen atoms, indicating that during annealing the hydroxyl groups of H40 form H-bonds with either carbonyl or another hydroxyl groups. The same H-bonds are also characteristic for the original H40 at room temperature. Moreover, the difference spectra are very similar to the difference spectrum for H40 recorded at room temperature and at 130 °C[34] (Figure 11B), indicating that during annealing some broken or bent −OH...−OH and/or −OH...O=C⟨ H-bonds rearrange their structure at room temperature. The rearrangement of the H-bond structure at an annealing temperature of 50 °C is very similar to that at 90 °C. The difference is only in the intensity of the difference bands, which correlate with the number of proton donors and acceptors involved in the process of rearrangement. Figure 7 shows that the H-bond rearrangement is more intense at lower annealing temperature, which is consistent with the results of DSC and rheological measurements.

3.1.4. XRD. The ordering of H40 structure was also confirmed by XRD measurements (Figure 8). The X-ray diffractogram of quenched H40 (denotation Q) exhibits a broad amorphous halo at around $2\theta = 17°$. The annealed sample (denotation A) has a much sharper amorphous halo than the quenched sample, whereas the position of the peak maximum is very similar in both X-ray patterns, $2\theta = 17.36°$, which corresponds to a distance of 0.516 nm. This distance was ascribed to the spacing between linear aliphatic polyester chains.[23] There are no other peaks that would indicate the presence of crystalline structure in the sample.

3.2. Characterization of Individual Fractions of Boltorn H40 HB Polyester. 3.2.1. Thermal Characterization. The existence of −OH...−OH H-bonds in annealed fractions F1 and F3 is indicated in their DSC thermograms by the endotherms at 98.5 °C ($\Delta H = 9.3$ J g^{-1}) and at 89.7 °C ($\Delta H = 8.9$ J g^{-1}), respectively (Figure 9).

3.2.2. FTIR Spectrometry. The changes in H-bond network structure due to heating the fractions are presented in difference spectra in Figure 10A. The changes are presented by the derivative bands, which are most significant in the stretching region of the vibration of hydroxyl and carbonyl groups.

A comparison of both difference spectra shows that the intensity of the bands in the difference spectrum of F3 is much higher, indicating that as the temperature is raised the number of broken/weakened H-bonds is higher in F3 than in F1. Both difference spectra also differ in the relative intensity of the bands in the carbonyl and hydroxyl stretching region. The relative amount of −OH...O=C⟨ H-bonds as compared to that of −OH...−OH H-bonds is higher in F3 than in F1.

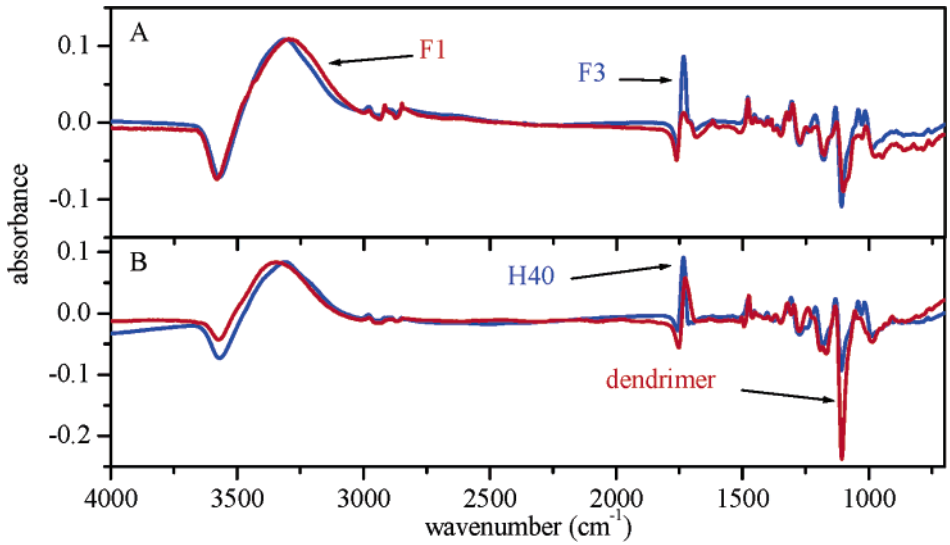

Figure 10. (A) Difference spectra of fractions F1 and F3. The scale factors are 4.0 for F1 (red curve) and 1 for F3 (blue curve). (B) Difference spectra of dendrimer and H40. The scale factors are 1.3 for dendrimer (red curve) and 1 for H40 (blue curve). The difference spectrum for each sample was obtained by the subtraction of the spectrum recorded at 130 °C from that recorded at room temperature. The difference spectra are scaled to the same intensity of the band due to the stretching vibration of H-bonded hydroxyl groups.

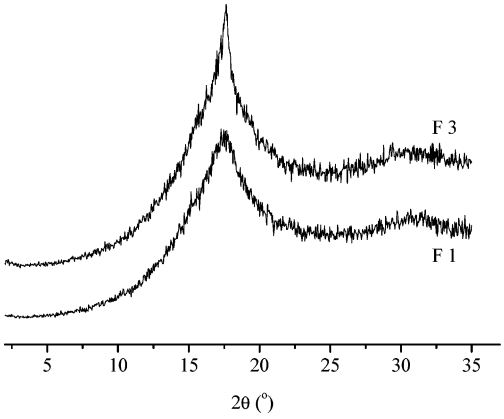

Figure 11. X-ray diffractograms of fractions F1 and F3 annealed at 80 °C for several days.

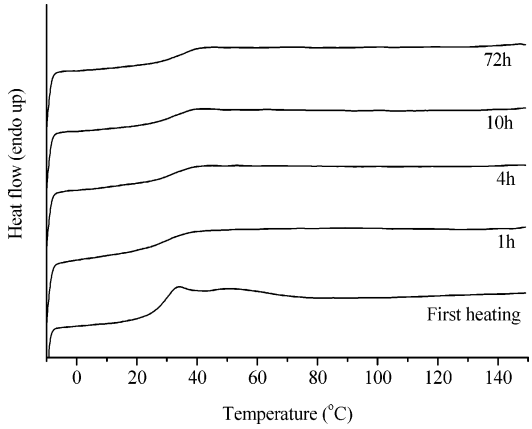

Figure 12. DSC curves of the original dendrimer (the first heating) and that annealed at 60 °C for various annealing times (1, 4, 10, and 72 h).

3.2.3. XRD. The X-ray patterns of both fractions show the same position of the center of the amorphous halo ($2\theta = 17°$), only that fraction F3 has sharper shape of the peak than fraction F1 (Figure 11).

3.3. Characterization of Dendrimer Based on Bis-MPA. 3.3.1. Thermal Characterization. The first heating DSC thermogram of the original dendrimer sample shows a broad endothermic transition, which is superimposed on the glass transition and extends up to 75 °C (Figure 12) and is ascribed to the cleavage of intermolecular H-bonds between terminal hydroxyl groups. After annealing the dendrimer at 60 °C for various annealing times (1, 4, 10, 72 h) the DSC traces of dendrimer show only a T_g and no exo- or endothermic transitions (Figure 12). Such a thermogram is obtained for H40 only when all hydroxyl groups are end-capped (not shown). According to these results, the dendrimer after annealing occupies such a molecular conformation that it does not allow H-bonding between end hydroxyl groups.

3.3.2. FTIR Spectrometry. The difference spectrum of dendrimer obtained from FTIR temperature measurements shows similar features to the difference spectrum of H40 (Figure 10B). The lower intensity of the bands in the difference spectrum of the dendrimer compared to H40 indicates that during heating the number of broken and/or weakened H-bonds is lower in the dendrimer than in H40. A comparison of the relative intensities between the bands representing the changes in the stretching vibration of hydroxyl and carbonyl groups in both difference spectra show that the relative amount of −OH...O=C⟨ H-bonds compared to −OH...−OH H-bonds is higher in the dendrimer than in H40. The same was also concluded from a comparison of dendrimer and H40 FTIR spectra recorded at room temperature.

3.3.3. XRD. The X-ray diffractograms of the quenched (Q) and annealed (A) dendrimer (Figure 13) show no changes in either the position or the shape of the broad amorphous halo meaning that annealing does not induce ordering of the dendrimer structure.

The shape of the amorphous halo in the X-ray pattern of the dendrimer is the same as that of the quenched H40 (Figure 8). These results indicate a disordered or amorphous structure of dendrons emanating from the core, which agrees with the prominent glass transition in its DSC trace. The corresponding distance calculated from the maximum of the broad peak ($2\theta = 17°$) is comparable to that of the H40 polyester.

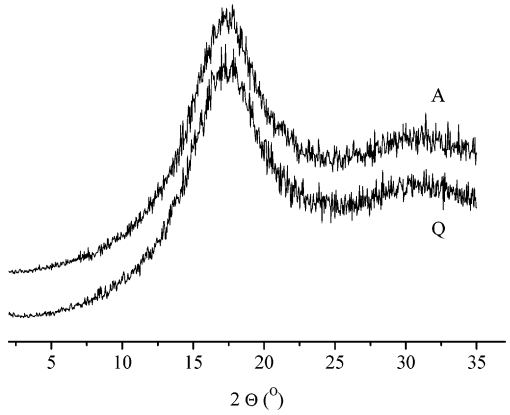

Figure 13. X-ray diffractograms of quenched and annealed dendrimer. Q = quenched dendrimer; A = annealed dendrimer at 50 °C for 14 days.

4. Discussion

It is known that the H-bonding associated with the large number of hydroxyl groups in H40 is responsible for its solid-state and solution properties.[13,19−22,28,33] For an understanding of the effect of annealing on the H40 H-bond network rearrangement and consequently on its thermal and rheological properties, besides sample average composition, structure, $\overline{DB}$, and molar mass, also the dependence of these parameters on molar mass should be known. These parameters are the key factors for proposing the H-bond network structure and, consequently, the relationship between the structure and properties of H40.

Therefore, we analyzed two individual fractions of H40 (F1 and F3) obtained by preparative SEC[18] which significantly differ in molar mass and $\overline{DB}$. The fractions are well-defined with respect to the above-mentioned parameters and therefore could be considered model compounds (Table 1). The fraction F1 has a $\overline{DP}_n$ (61.5) comparable to that of its ideal dendrimer analogue (61) and the highest $\overline{DB}$ (0.37) among all the fractions. It contains mostly HB structures with a core molecule. On the average, for every 5.7 incorporated bis-MPA units, one is dendritic. Among all the fractions, fraction F3 has the lowest $\overline{DP}_n$ (16.5), the lowest $\overline{DB}$ (0.32), and the highest content of HB structures without a core molecule. On average, the sequence consists of no more than one dendritic unit for 7.4 incorporated bis-MPA units. Because of its low molar mass and low $\overline{DB}$, F3 has a more open and linear structure that can easily permit the branches of a given molecule to penetrate into the interior of the neighboring molecule. By this means the hydroxyl groups in long linear sequences form multiple intermolecular H-bonds with either carbonyl or hydroxyl groups of other linear sequences. This is further supported by the fact that F3 on the average contains only two dendritic units per four branches in molecules with a core molecule and two dendritic units per three branches in molecules without a core, which means that some of the branches are composed solely of linear sequences. Long linear sequences can establish more intermolecular H-bond contacts resulting in their closer proximity and consequently in more ordered and compact H-bond structure (Figure 11).[13,28]

The thermal stability of the H-bond network formed after annealing is much better than that of the original sample, which was proved by the SEC-MALS results of the annealed fractions in solvents DMAc/LiCl or THF/methanol mixture. The H-bond network cannot be completely disrupted either by the thermal pretreatment of samples or by the addition of LiBr to DMAc or methanol to THF. F3 had the lowest level of broken H-bonds.[18]

To demonstrate that linear sequences in the HB structure are responsible for the observed ordering of the structure, which influences the thermal and rheological properties of H40, the dendrimer analogue of H40 was also analyzed. The dendrimer consist of the same bis-MPA building blocks as H40. However, in contrast to H40, the dendrimer has an ideally branched structure with no linear sequences, and therefore its DB equals 1.

The hydroxyl groups in the terminal repeat units of the original dendrimer sample are H-bonded to carbonyl as well as to another hydroxyl groups (Figures 12 and 13). During annealing of the dendrimer at 60 °C the intermolecular H-bonds between terminal hydroxyl groups are to a large extent disrupted. The outer dendrimer layer with the end hydroxyl groups most probably folds back toward its interior, resulting in a globular structure in which the end hydroxyl groups are preferably intramolecularly H-bonded to the interior carbonyl groups. Therefore, the DSC traces of dendrimer after annealing for various annealing time show no endothermic transitions. Since the dendrimer does not consist of linear repeat units the annealing does not induce the ordering of its structure (Figure 13). Such results are evidence that linear sequences in the HB structure of H40 are responsible for the thermal and rheological properties of H40.

Taking all the presented results into account, it can be concluded that the intermolecular H-bond network in the original Boltorn H40 can be successfully broken by preheating the sample to a temperature about 100−120 °C above its T_g (31 °C). Therefore, thermally pretreated Boltorn H40 behaves like a Newtonian fluid.[13,25,26] On the other hand, during the annealing of Boltorn H40 at temperatures above its T_g, e.g. between 50 and 100 °C, a more ordered and thermally stable H-bond network microstructure is formed than that found in the original sample.

From the comparison of the FTIR difference spectrum of H40 before and after annealing (Figure 7) with that of H40 obtained by subtraction of the spectra recorded at 130 °C and at room temperature (Figure 10B), we can see that the number of H-bonds between hydroxyl and carbonyl groups increases considerably during annealing. Namely, the intensity ratio of the H-bonded carbonyl to the hydroxyl stretching band is higher in the difference spectrum obtained by annealing than in the difference spectrum obtained by heating. The high relative amount of −OH...O=C⟨ compared to −OH...−OH H-bonds in the annealed H40 can be explained by the fact that during annealing long linear sequences organize into more ordered and thermally stable H-bond network through multiple intermolecular H-bond interactions. The presented results indicate that the observed thermal and rheological properties of H40 are governed especially by sample composition, i.e., degree of branching and molar mass. The importance of these structural features in determining the properties of HB polymers has also been recently reported for HB aliphatic polyethers.[49]

In addition, the results obtained for fractions F1 and F3 can be compared to those of different generation Boltorn HX HB polyesters. It is known that the sharpness of the amorphous halo in X-rays patterns of Boltorn polyesters strongly increases with decreasing generation.[23] Besides, the FTIR difference spectra of Boltorn polyesters show that the number of broken and/or weakened H-bonds during heating increases with decreasing generation. Boltorn H20 and H30 have a lower $\overline{DP}_n$ than F3 and lower (H20) or comparable (H30) $\overline{DB}$ to that of F3. So, a high degree of intermolecular H-bond interaction between linear sequences can be expected, as in F3. We believe that the highly ordered structures[23] and shear-thinning behavior of lower generation Boltorn HX polyesters are a consequence not only of the intermolecular interactions between the hydroxyl groups on the periphery[25,26] but also of the multiple H-bond intermolecular interactions of the linear sequences. Stronger H-bond interactions of the low-generation poly(bis-MPA) HB polyesters are also reflected in the steeper slopes along the low molar mass part of the log η vs log M relationship[13] and in their greater activation energies of flow,[25] conductivity, and γ-relaxation.[32]

5. Conclusion

The thermal and rheological properties of Boltorn H40 HB polyester were studied dependent on annealing temperature and annealing time. It was shown that annealing of Boltorn HB polyester H40 above its glass transition temperature significantly affects its thermal and rheological properties. The kinetics of H-bond formation was followed by measuring the H-bond cleavage enthalpy of annealed H40. The process of H-bond formation is similar to the process of crystallization, and its kinetics can be adequately described by the crystallization kinetics. The cleavage enthalpy is a linear function of the logarithm of annealing time. The sample glass transition temperature is almost unaffected by the annealing process, whereas the heat capacity at the glass transition decreases with increasing cleavage enthalpy. At the beginning of the annealing process, the melt exhibits only viscous behavior at higher temperatures (80 and 90 °C) or predominantly viscous behavior at lower temperatures (60 and 70 °C). Because of the formation of H-bonds during annealing, the elastic contribution to the viscoelastic response of H40 increases with increasing annealing time at all annealing temperatures.

During annealing the amorphous H40 develops a more ordered and thermally stable H-bond network structure. By comparing the XRD and FTIR results of H40 to those of its fractions and to the dendrimer analogue, we conclude that during annealing of H40 the linear sequences in the hyperbranched structure form multiple H-bond contacts through −OH...O=C⟨ and/or −OH...−OH H-bonds. The highest degree of such interactions was found for the low molar mass species, which have an open structure and the longest average length of linear sequences between branch points.

The degree of branching and the molar mass have been found to be the main structural features of HB poly(bis-MPA) polyesters influencing the formation of the H-bond network, its type and strength, and, consequently, the thermal and rheological properties of HB poly(bis-MPA) polyesters as well.

Acknowledgment. The authors gratefully acknowledge the financial support of the Ministry of Education, Science and Sport of the Republic Slovenia (program P2-145) and the participation in the EU NoE Nanofunpoly. The authors are also grateful to Prof. Dr. Andreas Hult, Royal Institute of Technology, Stockholm, Sweden, for supplying the fourth-generation dendrimer sample based on 2,2-bis(methylol)propionic acid.

References and Notes

(1) Fréchet, J. M. J. *Science* **1994**, *263*, 1710.
(2) Hawker, C. J.; Farrington, P. J.; Mackay, M. E.; Wooley, K. L.; Frechet, J. M. J. *J. Am. Chem. Soc.* **1995**, *117*, 4409.
(3) Kim, Y. H.; Webster, O. W. *Macromolecules* **1992**, *25*, 5561.
(4) Mourey, T. H.; Turner, S. R.; Rubinstein, M.; Fréchet, J. M. J.; Hawker, C. J.; Wooley, K. L. *Macromolecules* **1992**, *25*, 2401.
(5) Uppuluri, S.; Keinath, S. E.; Tomalia, D. A.; Dvornic, P. R. *Macromolecules* **1998**, *31*, 4498.
(6) Dvornic, P. R.; Uppuluri, S.; Tomalia, D. A. *Polym. Mater. Sci. Eng.* **1995**, *73*, 131.
(7) Uppuluri, S.; Morrison, F. A.; Dvornic, P. R. *Macromolecules* **2000**, *33*, 2551.
(8) Farrington, P. J.; Hawker, C. J.; Fréchet, J. M. J.; Mackay, M. E. *Macromolecules* **1998**, *31*, 5043.
(9) Kim, Y. H.; Webster, O. W. *J. Am. Chem. Soc.* **1990**, *112*, 4592.
(10) Wooley, K. L.; Hawker, C. J.; Lee, R.; Fréchet, J. M. J. *Polym. J.* **1994**, *26*, 187.
(11) Malmström, E.; Johansson, M.; Hult, A. *Macromolecules* **1995**, *28*, 1698.
(12) Turner, S. R.; Voit, B. I.; Mourey, T. H. *Macromolecules* **1993**, *26*, 4617.
(13) Luciani, A.; Plummer, C. J. G.; Nguyen, T.; Garamszegi, L.; Månson, J.-A. E. *J. Polym. Sci., Part B: Polym. Phys.* **2004**, *42*, 1218.
(14) Malmström, E.; Hult, A. *Macromolecules* **1996**, *29*, 1222.
(15) Magnusson, H.; Malmström, E.; Hult, A. *Macromolecules* **2000**, *33*, 3099.
(16) Burgath, A.; Sunder, A.; Frey, H. *Macromol. Chem. Phys.* **2000**, *201*, 782.
(17) Komber, H.; Ziemer, A.; Voit, B. *Macromolecules* **2002**, *35*, 3514.
(18) Žagar, E.; Žigon, M. *Macromolecules* **2002**, *35*, 9913.
(19) Žagar, E.; Žigon, M. *J. Chromatogr. A* **2004**, *1034*, 77.
(20) Garamszegi, L.; Nguyen, T. Q.; Plummer, C. J. G.; Månson, J.-A. E. *J. Liq. Chromatogr. Relat. Technol.* **2003**, *26*, 207.
(21) Pruthtikul, R.; Coleman, M. M.; Painter, P. C. *Macromolecules* **2001**, *34*, 4145.
(22) Xu, M.; Yan, X.; Cheng, R.; Yu, X. *Polym. Int.* **2001**, *50*, 1338.
(23) Rogunova, M.; Lynch, T.-Y. S.; Pretzer, W.; Kulzick, M.; Hiltner, A.; Baer, E. *J. Appl. Polym. Sci.* **2000**, *77*, 1207.
(24) Nunez, C. M.; Chiou, B.-S.; Andrady, A. L.; Khan, S. A. *Macromolecules* **2000**, *33*, 1720.
(25) Hsieh, T.-T.; Tiu, C.; Simon, G. P. *Polymer* **2001**, *42*, 1931.
(26) Hsieh, T.-T.; Tiu, C.; Simon, G. P. *Polymer* **2001**, *42*, 7635.
(27) Malmström, E.; Johannson, M.; Hult, A. *Macromol. Chem. Phys.* **1996**, *197*, 3199.
(28) Hult, A.; Malmström, E.; Johannson, M. In Salamone, J. C., Ed.: *Polymeric Materials Encyclopedia*; CRC Press: Boca Raton: FL, 1996.
(29) Hedenqvist, M. S.; Yousefi, H.; Malmström, E.; Johansson, M.; Hult, A.; Gedde, U. W.; Trollsås, M.; Hedrick, J. L. *Polymer* **2000**, *41*, 1827.
(30) Malmström, E.; Liu, F.; Boyd, R. H.; Hult, A.; Gedde, U. W. *Polym. Bull. (Berlin)* **1994**, *32*, 679.
(31) Malmström, E.; Hult, A.; Gedde, U. W.; Liu, F.; Boyd, R. H. *Polymer* **1997**, *38*, 4873.
(32) Zhu, P. W.; Zheng, S.; Simon, G. *Macromol. Chem. Phys.* **2001**, *202*, 3008.
(33) Johansson, M.; Glauser, T.; Jansson, A.; Hult, A.; Malmström, E.; Claesson, H. *Prog. Org. Coatings* **2003**, *48*, 194.
(34) Žagar, E.; Grdadolnik, J. *J. Mol. Struct.* **2003**, *658*, 143.
(35) Hawker, C. J.; Lee, R.; Fréchet, J. M. J. *J. Am. Chem. Soc.* **1991**, *113*, 4583.
(36) Hölter, D.; Burgath, A.; Frey, H. *Acta Polym.* **1997**, *48*, 30.
(37) (a) Bertie, J. E.; Eisel, H. H. *Appl. Spectrosc.* **1985**, *39*, 392. (b) Bertie, J. E.; Lan, Z. *J. Chem. Phys.* **1996**, *105*, 8502.
(38) Ho, C. H.; Vu-Khanh, T. *Theor. Appl. Fract. Mech.* **2003**, *39*, 107.
(39) Hutchinson, J. M.; Kumar, P. *Thermochim. Acta* **2002**, *391*, 197.
(40) Lee, Y. D.; Phillips, P. J. *J. Appl. Polym. Sci.* **1990**, *40*, 263.

(41) Skoglund, P.; Fransson, Å. *Polymer* **1998**, *39*, 1899.
(42) Hadjichristidis, N.; Pispas, S.; Floudas, G. A. *Block Copolymers*; John Wiley & Sons: New York, 2003; pp 313−334.
(43) Fatou, J. G. In *Encyclopedia of Polymer Science and Engineering;* Mark, H. F., Bikales, N. M., Overberger, C. G., Menges, G., Eds.; John Wiley and Sons: New York, 1989; Suppl. Vol., pp 231−296.
(44) Booth, A.; Hay, J. N. *Polymer* **1971**, *12*, 365.
(45) Strobl, G. R.; Engelke, T.; Maderek, E.; Urban, G. *Polymer* **1983**, *24*, 1585.
(46) Huskić, M. *J. Appl. Polym. Sci.* **1996**, *60*, 1741.
(47) Shalaby, S. W. In *Thermal Characterization of Polymeric Materials*; Turi, E. A., Ed.; Academic Press: Orlando, FL, 1981; p 255.
(48) Hanselmann, R.; Hölter, D.; Frey, H. *Macromolecules* **1998**, *31*, 239.
(49) Magnusson, H.; Malmström, E.; Hult, A.; Johansson, M. *Polymer* **2002**, *43*, 301.

MA0475434